GEOPHYSICAL RESEARCH LETTERS, VOL. 25, NO.15, PAGES 2929-2932, AUGUST 1, 1998

# Bipolar electrostatic structures in the shock transition region: Evidence of electron phase space holes

S. D. Bale[1], P. J. Kellogg[2,3], D. E. Larson[1], R. P. Lin[1,4], K. Goetz[2], and R. P. Lepping[5]

**Abstract.** We present observations of intense, bipolar, electrostatic structures in the transition region of the terrestrial bow shock from the Wind spacecraft. The electric field signatures are on the order of a tenth of a millisecond in duration and greater than 100 mV/m in amplitude. The measured electric field is generally larger on the smaller dipole antenna, indicating a small spatial size. We compare the potential on the two dipole antennas with a model of antenna response to a Gaussian potential profile. This result agrees with a spatial scale determined by convection and gives a characteristic scale size of 2 - 7 $\lambda_d$. We interpret the observations as small scale convecting unipolar potential structures, consistent with simulations of electron phase space holes and discuss the results in the context of electron thermalization at strong collisionless shocks.

## 1. Introduction

Collisionless shocks must convert low entropy, upstream plasma flow into a sub-Alfvènic, high entropy state without the benefit of binary particle collisions. In the case of electron thermalization, wave-particle interactions have long been invoked as the heating agent and the electrostatic turbulence observed in the upstream, transition, and downstream regions of the terrestrial bow shock [*Rodriguez and Gurnett*, 1975] was proposed for this role. *Goodrich and Scudder* [1984] suggested that coherent DC fields dominate the electron heating, inflating phase space as the incident electrons move through the shock layer adiabatically. *Wygant et al.* [1987] observed intense, spikey electric fields near the shock and *Scudder et al.* [1986] showed that the plasma waves observed at one particular shock crossing were unable to account for the electron heating and suggested that the role of wave-particle interactions is to instead 'cool' the electron distribution by filling the phase space hole imposed by the Vlasov-Liouville mapping across the shock layer [*Hull et al.*, 1998].

In this letter, we present observations of intense, bipolar electric field signatures on the terrestrial bow shock ramp sampled by instruments on the Wind spacecraft. Similar observations have been made by Geotail in the plasma sheet boundary layer and bow shock [*Matsumoto et al.*, 1994; *Matsumoto et al.*, 1997], and in the auroral current regions [*Mozer et al.*, 1997; *Ergun et al.*, 1998]. The measured electric field is stronger on the shorter of two spin plane dipole antennas. Comparing the ratio of measured voltage to a model of antenna response, we conclude that the typical spatial size of the potential structures is a few Debye lengths. This agrees well with a spatial scale calculated by assuming that the structures are at rest, or slowly moving, in the convecting solar wind. We suggest that the observed structures are BGK modes known as electron phase space holes, and discuss this briefly in the context of collisionless shocks.

## 2. Analysis

Figure 1 shows the shock crossing at approximately 16:25 UT on October 20, 1997. Panel (a) shows data from the Thermal Noise Receiver (TNR) instrument of the WAVES experiment; an enhancement in very low frequency noise is present below roughly 20 kHz. In panel (b), data from the Time Domain Sampler (TDS) instrument of WAVES is shown. There are 14 triggered TDS waveform events during this shock crossing; this data will be discussed more below, but suffice it to notice the large amplitude of the electric fields. The data from the TNR instrument (panel a) is sampled from the same sensors, but is transformed and averaged on board. The lower three panels show the electron moment temperature, as calculated from Three Dimensional Plasma (3DP) instrument burst mode data, the 3DP solar wind bulk flow speed, and the magnetic field magnitude from the MFI instrument. Descriptions of the instruments on the Wind spacecraft are in the literature [*C. T. Russell*, 1995]. We will not analyze the shock structure in detail, and only note that the shock is high $\beta$, supercritical (magnetosonic Mach number $M \approx 9.5$) and quasi-perpendicular, as determined a lack of upstream ions and turbulence. The shock tangent angle

[1]Space Sciences Laboratory, University of California, Berkeley
[2]School of Physics and Astronomy, University of Minnesota, Minneapolis
[3]DESPA, Observatoire de Paris, Meudon, FRANCE
[4]Department of Physics, University of California, Berkeley
[5]NASA Goddard Space Flight Center, Greenbelt



Paper number 98GL02111.
0094-8534/98/98GL-02111$05.00

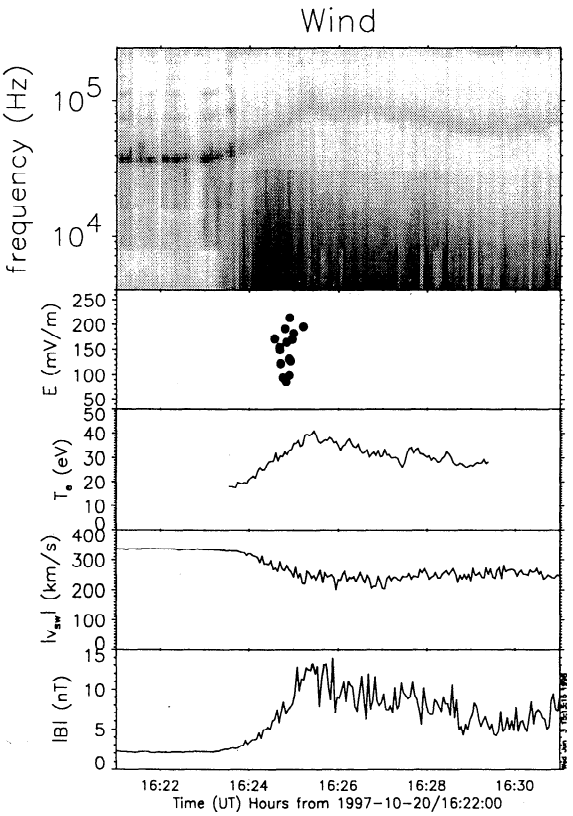


**Figure 1.** The shock crossing. The TNR spectrogram shows broadband wave activity below the electron plasma frequency in panel (a). Panel (b) shows the location and amplitude of the TDS waveform events. Panels (c)-(e) show electron temperature, solar wind speed, and magnetic field magnitude respectively.

$\Theta_{bn}$ was calculated by three different methods: minimum variance, velocity coplanarity, and with respect to a pressure scaled shock model. These methods all produced values of $\Theta_{bn}$ between 70° and 80°, verifying that the shock is indeed quasi-perpendicular.

Figure 2 shows two waveform events from the TDS instrument. The top two panels (a) are the electric field on the X and Y antennas respectively from an event at 16:24:59 UT. The TDS samples simultaneously on two orthogonal wire dipole antennas, of tip-to-tip lengths 100 m and 15 m, and returns peak-centered events of 2048 points; these events are buffered on the spacecraft and sorted by peak amplitude of the $X$ antenna signal. The largest amplitude events above a hardware threshold of $\approx 0.05\ mV/m$ are telemetered preferentially. Electric field is calculated by dividing the potential difference by an effective length ($l_x \approx 43m$ and $l_y \approx 4.7m$). The first TDS event shows the characteristic signature of these events: a large bipolar electric field spike in the center of the sampling interval. An important point is that the electric field of the spike is generally larger on the smaller dipole antenna; the average maximum electric field for the 14 events is 153 mV/m on the small dipole. The relative phase of the X and Y components varies and is discussed below. The second TDS event (panel (b)) shows bipolar spikes embedded in a nonlinear wave field; again the spikes are larger in amplitude on the small antenna. Examination of a concomitant magnetic channel during other events shows no corresponding signal, hence we identify the events as electrostatic. These events all occur near the magnetic overshoot of the shock structure, between 16:24:33 and 16:25:28 UT, as indicated by the second panel of Figure 1. These 14 events add up to $14 \times 17\ msec \approx 238\ msec$ of data during this 54 second interval. Since the instrument buffer holds 20 events; any other electric fields during this time, or afterwards, were of smaller amplitude.

The bipolar electric field signature indicates a unipolar electric potential. Assuming a Gaussian potential profile $\phi(x) = \phi_0\, e^{-x^2/\Lambda^2}$, of characteristic width $\Lambda$, the dipole antenna response can be calculated as the difference between the average potential on each monopole element of length $L$.

$$\Delta V = \left(\frac{1}{L}\int_0^L dy\ \phi(y) - \frac{1}{L}\int_{-L}^0 dy\ \phi(y)\right) \qquad (1)$$

For the Gaussian potential $\phi(x)$ displaced from the origin by $x_0$, equation (1) can be written

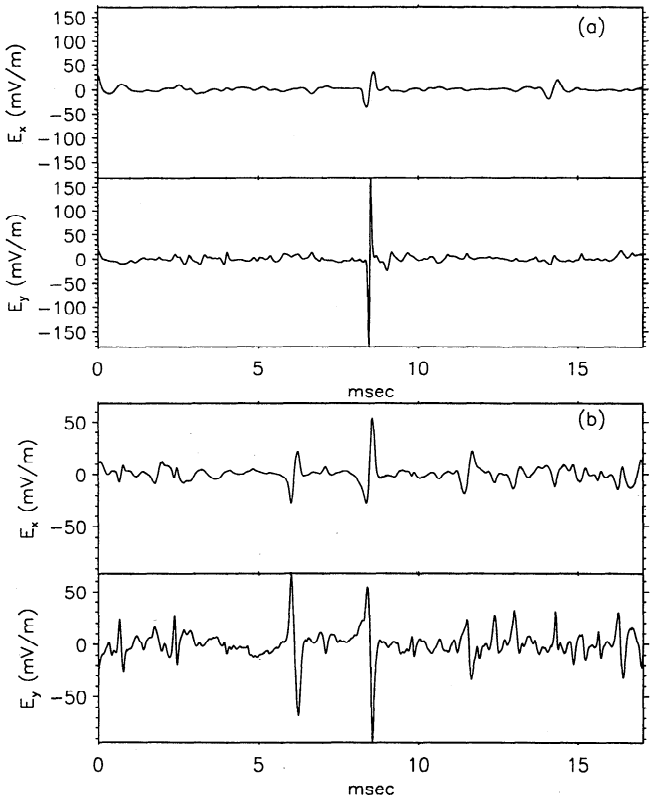


**Figure 2.** The top two panels (a) show the $X$ and $Y$ components of a TDS waveform event. The intense bipolar spike is centered in the event and much larger on the shorter ($Y$) antenna. The bottom two panels (b) show another event with several spikes embedded in a weaker, nonlinear wave field.

$$\Delta V = \phi_0 \frac{\Lambda}{L} \left( \int_{-\frac{x_0}{\Lambda}}^{\frac{L-x_0}{\Lambda}} dy\, e^{-y^2} - \int_{\frac{-L-x_0}{\Lambda}}^{\frac{-x_0}{\Lambda}} dy\, e^{-y^2} \right) \quad (2)$$

which can be expressed as a sum of error functions.

The solid line in Figure 3 shows the ratio $\Delta V_y/\Delta V_x$ of the calculated response for the two antennas, with monopole lengths $L_x = 50\ m$ and $L_y = 7.5\ m$ as a function of the characteristic width of the Gaussian potential $\Lambda$ at small displacement $x_0 = 0.05\ \lambda_d$; we use the average Debye length of the events $\lambda_d = 6.8m$ as calculated from local electron density and temperature measurements. Although the measured potential goes to zero as $x_0$ goes to zero, the ratio of potentials remains finite. For the observed voltage ratio $\Delta V_y/\Delta V_x$ to be large, the scale size of the potential profile must be only a few Debye lengths. The ratio of voltages does not show any good correlation with the magnetic field direction; this is not surprising as the characteristic timescale of these events ($\Delta t \approx 0.1$ msec) is much less than an electron cyclotron period ($\tau_{ce} \approx 3.5$ msec). The ambient magnetic field is probably only important in as much as it controls the direction of currents in the shock front, however, the small data statistics of this one shock crossing may prevent us from seeing any correlation.

Assuming that the structures are at rest in the convecting solar wind, the sample time of the measurement can be converted to a spatial scale $\Delta x = v_{sw}\ \Delta t$. A typical temporal width for an event is 0.1 msec, which becomes $x \approx 4\ \lambda_d$ for a slowed solar wind speed of 265 km/s and Debye length of 6.8 m. We have scaled of the characteristic width of 14 events observed during this bow shock crossing using the *in situ* solar wind speed and Debye length. For each event, the ratio $|\Delta V_y|/|\Delta V_x|$ is obtained at the maximum and minimum potential value of the $Y$ antenna signal and the solid dot is the average. These values are overplotted on Figure 3, with the maximum and minimum potential potential ratios giving the limits of the error bars. The values agree well with the theoretical ratio of responses assuming a Gaussian potential. The agreement may be even better if approximately $1\lambda_d$ is added to the convection scale; this would imply a typical velocity of $\lambda_d/\Delta t \approx$ 67 km/s with respect to the solar wind.

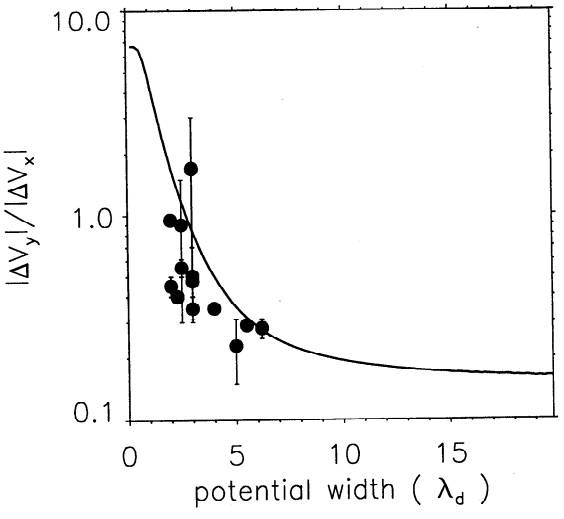


**Figure 3.** The ratio of antenna responses against potential scale $\Lambda$, in units of local average Debye length. The solid line shows the theoretical ratio of measured voltage on the Y and X antennas. The solid dots are the mean ratio of voltages plotted against a convection scale size determined by $\Delta x = v_{sw}\Delta t$; the error bars show the minimum and maximum voltage ratios.

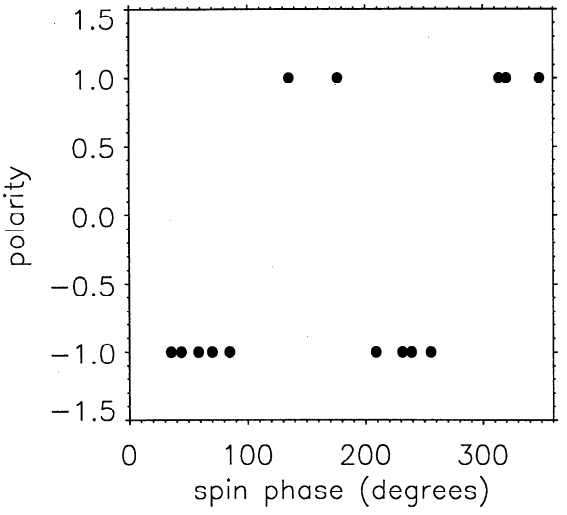


**Figure 4.** Polarity against spin phase. $Signum(E_x) * signum(E_y)$ changes sign four times during one spin; this indicates a one dimensional unipolar potential structure. Both the solar wind and IMF directions are near zero spin phase.

Figure 4 shows the polarity vs. spin phase; polarity is just $signum(E_x) * signum(E_y)$ at the peak of each bipolar spike and spin phase is the angle between the $X_{gse}$ direction and the spacecraft $X$ axis. As discussed by *Matsumoto et el.* [1994], the polarity changes sign four times per spin and indicates a one dimensional, unipolar potential structure moving past the spacecraft, consistent with the above results. During this interval, the IMF is directed nearly radially, so that it is difficult to know if it is the IMF or solar wind direction that orders the data.

## 3. Interpretation

We have shown that very intense, bipolar electric field spikes are present in the transition region of the bow shock. By comparing the measured potential on two antennas of different length, we have determined that the responsible potential structures have characteristic scales on the order of a few Debye lengths. This is consistent with the scale size determined by assuming $\Delta x = v_{sw}\ \Delta t$ and implies that the structures are at rest

or slowly moving in the solar wind frame. These bipolar structures are similar, though more intense, to waveforms observed in the geomagnetic tail by the Geotail spacecraft [*Matsumoto et al.*, 1994]. Those data have been shown to be consistent with signature of an electron phase space hole [*Matsumoto et al.*, 1994; *Omura et al.*, 1994] generated by a two stream instability with a large beam to background density ratio. Similar, though more intense, electric fields signatures have been observed in the auroral region [*Mozer et al.*, 1997; *Ergun et al.*, 1998] on field lines supporting downward current. Phase space holes are stable solutions in the BGK formalism, and represent a dearth of electrons in an area of phase space on the order of $\lambda_d$ by $v_{th}$ [*Bernstein et al.*, 1957]. As such, they may play a role in maintaining finite resistivity in a plasma, as they represent clumps of positive charge that may scatter ions and in this way support the existence of a parallel electric field.

The theory of electron thermalization by DC fields at collisionless shocks [*Goodrich and Scudder*, 1984; *Scudder et al.*, 1986; *Hull et al.*, 1998] predicts an electron phase space hole in the downstream distribution function, in the shape of a nearly isotropic ellipse in velocity space, of size $v_\phi = \sqrt{2e[\phi_{HT}]/m}$, where $[\phi_{HT}]$ is the cross-shock deHoffman-Teller potential. A polytropic assumption gives $e[\phi_{HT}] = \gamma_e/(\gamma_e - 1)[kT_e]$ which gives $v_\phi \approx \sqrt{2}\, v_{th}$ for our shock assuming $\gamma_e = 2$. It may be that our observations are the signature of electron phase space modification by the DC fields at the shock or the nonlinear evolution of a current-driven instability. A recent simulation [*Saeki and Genma*, 1998] has shown that an electron hole can decay by coupling to soliton modes and breaking into several smaller holes. This may be what is observed in the multiple spike events, with the end result being a very nonlinear wave field. It should be noted that the early spectral density measurements of electrostatic turbulence at the shock [e. g. *Rodriguez and Gurnett*, 1975] may merely indicate the spectral content of impulsive electric fields; hence, the relevance of linear wave modes in this region should be reexamined.

**Acknowledgments.** We thank R. E. Ergun and A. J. Klimas for interesting discussions. Work at UC Berkeley is supported by NASA grant NAG5-2815 to the University of California.

## References

Bernstein, I. B., J. M. Greene, and M. D. Kruskal, Exact nonlinear plasma oscillations, *Phys. Rev.*, *108*, 546, 1957.

Ergun, R. E., et al., FAST satellite observations of large-amplitude solitary structures, Geophys. Res. Lett., *25*, 2041, 1998.

Goodrich, C. C., and J. D. Scudder, The adiabatic energy change of plasma electrons and the frame dependence of the cross-shock potential at collisionless magnetosonic shock waves, J. Geophys. Res., *89*, 6654, 1984.

Hull, A. J., et al., Electron heating and phase space signatures at strong and weak quasi-perpendicular shocks, J. Geophys. Res., 2, 2041, 1998.

Matsumoto, H., et al., Electrostatic solitary waves (ESW) in the magnetotail: BEN waveforms observed by Geotail, Geophys. Res. Lett., *21*, 2919, 1994.

Matsumoto, H., et al., Plasma waves in the upstream and bow shock regions observed by Geotail, *Adv. Space Res.*, *20*, 683, 1997.

Mozer, F. S., et al., New features of time domain electric-field structures in the auroral acceleration region, Phys. Rev. Lett., *79*, 1281, 1997.

Omura, Y., H. Kojima, and H. Matsumoto, Computer simulation of electrostatic solitary waves: A nonlinear model of broadband electrostatic noise, Geophys. Res. Lett., *21*, 2923, 1994.

Rodriguez, P., and D. A. Gurnett, Electrostatic and electromagnetic turbulence associated with the earth's bow shock, J. Geophys. Res., *80*, 19 1975.

Russell, C. T., Ed., The Global Geospace Mission, Kluwer Academic Press, Dordrecht, 1995.

Scudder, J. D., et al.,The resolved layer of a collisionless, high $\beta$, supercritical, quasi-perpendicular, shock wave: 3. Vlasov electrodynamics, J. Geophys. Res., *91*, 11,075, 1986.

Saeki, K., and H. Genma, Electron-hole disruption due to ion motion and formation of coupled electron hole and ion-acoustic soliton in a plasma, Phys. Rev. Lett., 80, 1224, 1998.

Wygant, J. R., M. Bensadoun and F.S. Mozer, Electric field measurements at subcritical, oblique bow shock crossings, J. Geophys. Res., *92*, 11,109 1987.

S. D. Bale, D. E. Larson, and R. P. Lin, Space Sciences Laboratory, University of California, Berkeley, CA, 94720-7450 USA (email: bale@ssl.berkeley.edu)

K. Goetz and P. J. Kellogg, School of Physics and Astronomy, University of Minnesota, Minneapolis, MN, 55455 USA

R. P. Lepping, Laboratory for Extraterrestrial Physics, Code 690, NASA/GSFC, Greenbelt, MD 20771 USA

(Received April 14, 1998; revised June 9, 1998; accepted June 11, 1998.)